

Probing the morphology and tribo-response of nanostructured fluid films for personal care applications

G. Haugstad* and A Avery**

*University of Minnesota, Minneapolis, Minnesota, USA, haugs001@umn.edu

**Unilever Research, Port Sunlight, United Kingdom

ABSTRACT

A methodology is presented for probing silicone-based polymer-surfactant complex films a few nanometers in thickness with atomic force microscopy (AFM). The films include 2D regions of liquid character interspersed in regions of solid character. Images in dynamic regimes of net repulsive compared to net attractive interaction show remarkable differences, and are compared with contact mode images to help elucidate contrast mechanisms. Approach-retract cycles are explored in each regime to develop essential understandings of probe-film interaction. Highly selective liquid transport up the AFM tip is discovered and utilized diagnostically to reveal intriguing aspects of film morphology and dynamics.

Keywords: complex fluid, polydimethyl siloxane, CTAC, phase imaging, force volume

1 INTRODUCTION

Polymer/surfactant thin-film complexes are important components in “soft interface” technologies, notably in the personal care industry. Important components include silicone oils and cationic surfactants. Macroscale testing of tribological behavior has suggested a synergistic performance of silicone and surfactant. Improved mechanistic understandings are sought, however, including information on 2D film morphology spanning from millimeter to nanometer scales, as well as film thickness and tribological response resolved to the nanoscale; the latter includes an understanding of how 1D to 3D confinement affects tribological response. AFM is uniquely capable of probing nanoscale structure-property relationships in a nondestructive fashion and under conditions of interest to applications, including controlled gaseous (e.g., humidity) and liquid environments and over a range of temperatures in which soft condensed matter may exhibit crystalline, glassy, rubbery or liquid behavior.

The present study applies AFM in both quasistatic (“contact”) and dynamic (“tapping”) modes of operation, to examine complex films of (polydimethyl siloxane, PDMS) and cetyl trimethyl ammonium chloride (CTAC) adsorbed to mica surfaces from aqueous emulsion. The atomically flat character of mica allows detailed examination of ultrathin film morphology, because measured variations in height do not stem from substrate topography. The negative

charge state of mica surfaces in aqueous environment, together with polar character, provides a well-defined model interface useful to fundamental studies as well as applications.

2 EXPERIMENTAL DETAILS

PDMS with bulk viscosity of 10^6 cS, and CTAC (16 carbon units) were co-deposited on freshly cleaved mica during one-hour exposures to aqueous emulsion formulation, followed by 30-second deionized water rinse and one-hour oven drying. Films were imaged within 24 hours of preparation, and repeatedly over a period of weeks without identifiable change. AFM was performed with two scanning probe microscopes: a Nanoscope III Multimode (Digital Instruments) operated in ambient conditions (RH=25-45%) and a PicoScan PicoSPM (Molecular Imaging) with PicoApex environmental chamber under controlled humidity. V-shaped, gold-coated Si_3N_4 cantilevers with nominal spring constant of 0.58 N/m and oxide-sharpened tips were used for contact mode and occasionally dynamic AFM. Rectangular diving-board silicon cantilevers with integrated silicon tips, either uncoated or aluminum-coated, were employed for dynamic AFM [1], including “intermediate” ($k=3$ N/m, Budget Sensors) and “stiff” ($k=42$ N/m, Olympus) versions with resonance frequencies of approximately 75 and 300 kHz, respectively. A range of driving amplitudes were employed to achieve free oscillation resonant amplitudes (A_0) in the 10-70 nm range. Drive frequencies at or slightly below resonance were employed along with variable drive and set point amplitudes to explore both net attractive and net repulsive regimes [1] as described further in the results.

3 RESULTS AND DISCUSSION

PDMS-CTAC complex films exhibit starkly different topography depending on the regime of dynamic imaging as exemplified in Figure 1. The data were acquired with a “stiff” cantilever driven at resonance. Both top and bottom images were acquired at the relatively “nonperturbative” set point amplitude ratio $A/A_0=0.9$ [1]. Drive amplitudes differed for the top and bottom images such that a relatively small free oscillation amplitude ($A_0=23$ nm) pertained to the top case and large ($A_0=70$ nm) to the bottom case. Domains of corresponding phase contrast are observed in both cases. Brighter regions correspond to greater height or

lower phase (under the enumeration that phase decreases to zero well below resonance and increases to 180° well above resonance).

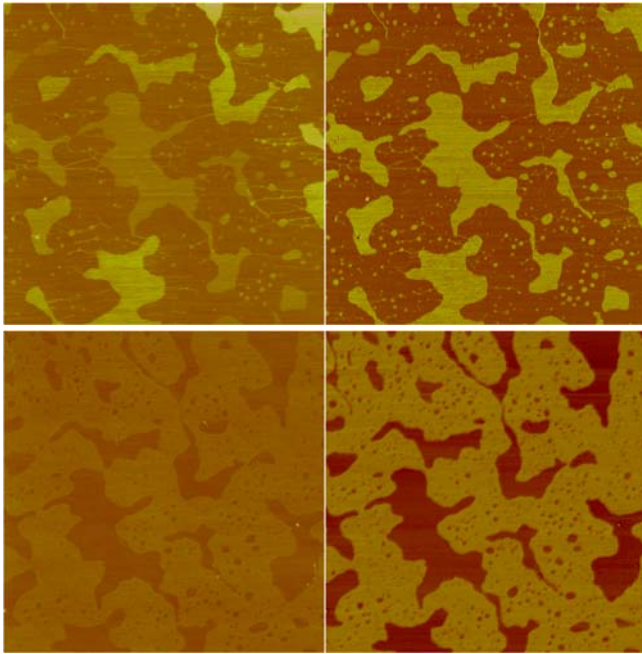


Figure 1. 5x5-micron height (left) and phase (right) images acquired using different drive amplitudes placing the system in the net attractive (top) and repulsive (bottom) regimes.

Both topographic and phase contrast invert between top and bottom sets of images in Figure 1. Islands of variably high surface elevation in the top height image (0.6-3.0 nm above surrounding “sea”) become uniformly low surface elevation “holes” in the bottom height image (0.3-0.4 nm below surroundings). Phase data acquired during approach-retract cycles determined that the top (bottom) case corresponded to the net attractive (repulsive) regime [1]. Within the energy dissipation interpretation of phase [1-2], brighter phase in the attractive regime (top right) corresponds to greater energy dissipation, whereas darker phase in the repulsive regime (bottom right) corresponds to greater energy dissipation. It is not uncommon in dynamic AFM that a given surface region exhibits higher energy dissipation in both attractive and repulsive regimes, resulting in inverted phase contrast [3].

What is remarkable in Figure 1 is the inversion of *height* contrast between top and bottom left in Figure 1. The height image in the repulsive regime is qualitatively similar to that observed in contact mode (not shown); under quasistatic contact the holes are uniformly 1.0-1.2 nm lower than the surrounding regions, compared to 0.3-0.4 nm lower under net repulsive dynamic interaction. Spatially resolved approach-retract curves in quasistatic contact mode were acquired in 32x32 locations (1024 data sets) to allow unambiguous force spectroscopy within the holes versus

that on the higher surroundings seen in contact mode images (not shown). A representative pair of these approach-retract curves are shown in Figure 2. The jump-to-contact in the “hole” regions occurs from vertical distances some 20 nm greater than the jump-to-contact on the surrounding regions. The jump-from-contact on the surrounding regions is purely vertical as conventionally observed on hard materials in air, whereas on the “holes” it exhibits a continuous character as known for example from AFM of polymer melts [4].

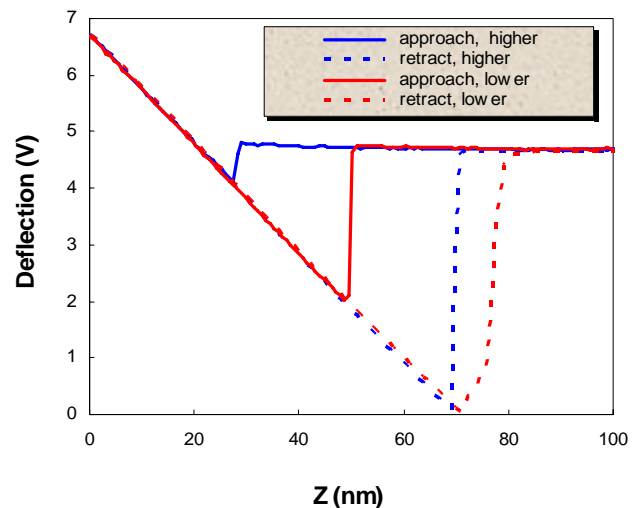


Figure 2. Quasistatic approach-retract curves comparing different characteristic behavior on surface regions exhibiting lower (“holes”) or higher (surrounding) surface elevation in topographic images acquired in contact mode or repulsive-regime dynamic mode imaging.

We interpret the behavior in quasistatic approach-retract curves on hole regions as a signature of liquidy character, involving substantial liquid necking between tip and sample during both jump-to and jump-from instabilities. We correspondingly interpret “holes” in both contact-mode and repulsive-regime dynamic mode as due to partial-to-full penetration of tip through islands of liquidy film. In parallel work, films cast from a formulation *lacking* the PDMS component (not shown) have very similar appearance to that of Figure 1 bottom left in terms of lateral size and shape of film domains, and exhibit two discrete surface elevations separated by 1.1-1.2 nm under repulsive dynamic imaging and ≈ 1.6 nm under quasistatic contact. This implies that while imaging the present films, nearly complete penetration of tip through liquidy domains to substrate occurs under quasistatic contact, and fractional penetration under dynamic repulsive interaction. The present “sea” is thus identified as a discontinuous monomolecular layer of CTAC. The frictional character (contact mode) of the identified CTAC layer is consistent whether PDMS-derived islands (Figure 1 top) or holes to mica (formulation lacking PDMS, not shown) are present between the CTAC domains.

While examining the effect of decreased set point amplitude A/A_0 on imaged topography in the attractive regime with an “intermediate” stiffness cantilever, a remarkable perturbation of film morphology was discovered that supports the above assignment of liquidy islands. After scanning submicron regions centered on “islands”, in the attractive regime at $A/A_0=0.5$, subsequent larger images at $A/A_0=0.9$ revealed substantial decreases in the apparent thickness of the domains. One such transformation is shown in Figure 3, height/phase images acquired in the attractive regime both before (top) and after perturbatively scanning a small subregion centered on the large island near the top of the image region. The “after” images reveal reduced apparent domain height and thus film thickness (1.6 nm above surrounding “sea”), and a corresponding sharp decrease in dissipative character as seen in phase that remains only slightly greater than the surrounding values. This suggests a “nano-drainage” phenomenon: capillary transport of liquidy components up the AFM tip.

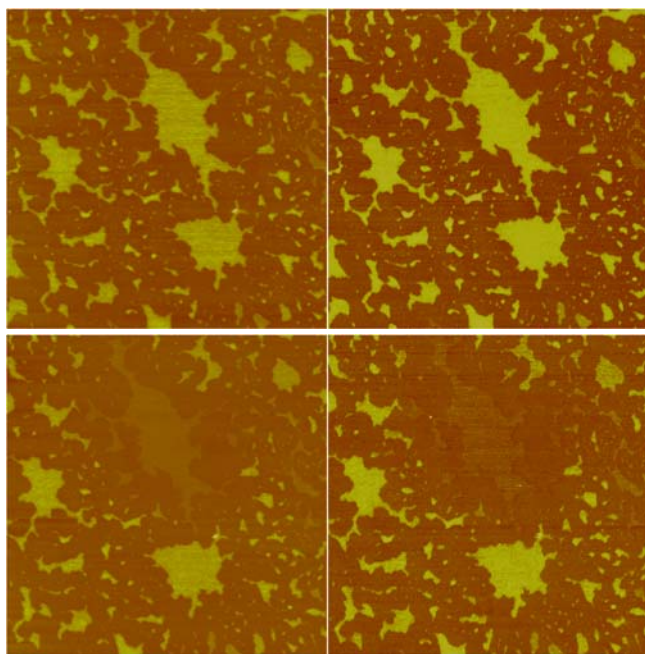


Figure 3. 15x15-micron height/phase images (left/right) acquired before (top) and after (bottom) perturbative scanning on the island near top center of each image.

It was reproducibly observed that any connected domains (“bays”) within a given island were uniformly drained, and that only a very small area of the island (much smaller than its entirety) need be scanned at $A/A_0=0.5$ to actuate the phenomenon, indicating surface transport over distances of *microns*. It was also noted that the more the island height was reduced by drainage, the closer the phase in the drained region approached that of the surrounding CTAC. The change of island height was uniform across any given (large) island, yet somewhat different from one

experiment to another. The remaining island always was approximately 1 nm or more in height above the surroundings (monomolecular layer of CTAC) and more uniform in height than the initial island. This suggests as few as two layers of CTAC remaining.

Capillary transport of small molecules to and from AFM tips in quasistatic contact is well-known and has been exploited in controlled nano-writing applications, otherwise known as “dip-pen nanolithography” [5]. To our knowledge, the present is the first report of capillary transport under intermittent interaction. Although our time-averaged cantilever deflection measurements during approach-retract curves (to continuous contact, not shown) revealed a slight average deflection towards sample at $A/A_0=0.5$, this deflection was very small compared to the oscillation amplitude. Thus intermittency was verified.

Immediately following the procedure assessed in Figure 3, the AFM tip was largely unchanged as evidenced by its approach-retract behavior in dynamic mode. After retracting and holding beyond sample engagement for at least 2 hours and as long as overnight, upon re-engagement the tip exhibited pronounced approach-retract hysteresis (increase of amplitude upon approach to interaction point, while driving precisely at resonance). This differed measurably and qualitatively from the behavior of the same tip upon first use and even immediately after the nano-drainage phenomenon. The observation was reproduced with several tips, suggesting the reproducible creation of a viscous “nanoprotuberance” at the end of each tip used for nano-drainage [6].

To better assess the possible composition of the liquidy islands and thus better understand nano-drainage, attractive-regime dynamic imaging was performed under variable humidity as exemplified in Figure 4. The characteristic thickness of islands was strongly and reversibly affected by the humidity, typically doubling or tripling in apparent thickness under high (60%) relative humidity. This suggests that water is incorporated into the islands under high humidity conditions.

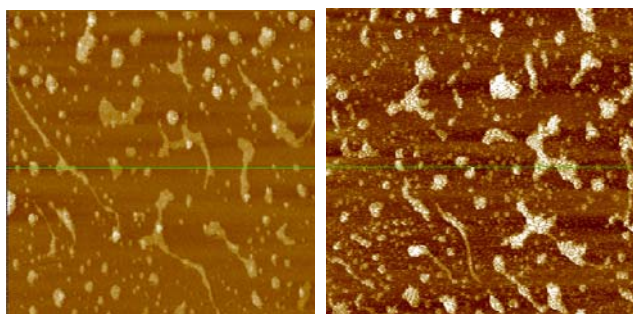


Figure 4. 5x5-micron height images acquired with dynamic AFM in the attractive regime at RH = 27% (left) and 60% (right). Islands at left range up to 5 nm, and at right up to 12 nm, in apparent thickness.

Given the observations of Figures 3-4, and complementary observations as described above, we suggest that the “drainable” islands incorporate a substantial amount of water. This in turn suggests that the islands, though absent in films cast from formulations lacking PDMS, contain hydrophilic molecules that intercalate with the hydrophobic PDMS such that water may be incorporated. This water presumably contributes as an entrainment fluid for capillary transport up the tip. Given time, excess water on the tip evaporates and large molecular-weight components remain, generating hysteretic, viscoelastic behavior [6] differing substantially from that of the bare tip.

4 CONCLUSIONS

Complex fluid films of the polymer PDMS and surfactant CTAC on mica comprise an island-sea morphology, wherein the sea is a contiguous monomolecular film of CTAC, and the islands incorporate not only PDMS but water and presumably CTAC. These islands exhibit a distinctive liquidy character that allows (a) tip penetration to near substrate under quasistatic contact-mode imaging and (b) less deep yet substantial tip penetration under repulsive-regime dynamic imaging. Only under attractive-regime dynamic imaging at large set point amplitude ratio ($A/A_0=0.9$) are the islands imaged as such. Under attractive dynamic imaging at intermediate set point amplitude ratio ($A/A_0=0.5$), capillary transport of liquidy components up the AFM tip takes place, under intermittent interaction.

REFERENCES

- [1] R. Garcia and R. Perez, Surf. Sci. Rep. 47, 197 (2002).
- [2] J. P. Cleveland, B. Anczykowski, A. E. Schmid, V. B. Elings, Appl. Phys. Lett. 72, 2613 (1998).
- [3] G. Haugstad and R. R. Jones, Ultramicroscopy 76, 77 (1999).
- [4] C. M. Mate and V. J. Novotny, J. Chem. Phys. 94, 8420 (1991).
- [5] R. D. Piner, J. Zhu, F. Xu, S. Hong, C. A. Mirkin, Science, 1999, 283, 661-663.
- [6] J. P. Aime, D. Michel, R. Boisgard and L. Nony, Phys. Rev. B 59, 2407 (1999).